Hindawi Publishing Corporation
EURASIP Journal on Wireless Communications and Networking
Volume 2010, Article ID 285714, 14 pages
doi:10.1155/2010/285714

Research Article

Joint Power Control, Base Station Assignment, and Channel Assignment in Cognitive Femtocell Networks

John Paul M. Torregoza,[1] Rentsen Enkhbat,[2] and Won-Joo Hwang[3]

[1] *Graduate School of Natural Sciences, Department of Computer Science, Inje University, Obang-dong, Gimhae, Gyeongnam 621-749, South Korea*
[2] *Department of Applied Mathematics, National University of Mongolia, Baga toiruu, Sukhbaatar district, Ulaanbaatar, 210646, Mongolia*
[3] *Graduate School of Engineering, Department of Information and Communications Engineering, Inje University, Obang-dong, Gimhae, Gyeongnam 621-749, South Korea*

Correspondence should be addressed to Won-Joo Hwang, ichwang@inje.ac.kr

Received 1 September 2009; Revised 15 December 2009; Accepted 29 January 2010

Academic Editor: Ismail Guvenc

Cognitive radio and femtocells are recent technology breakthroughs that aim to achieve throughput improvement by means of spectrum management and interference mitigation, respectively. However, these technologies are limited by the former's susceptibility to interference and the latter's dependence on bandwidth availability. In this paper, we overcome these limitations by integrating cognitive radio and femtocell technology and exploring its feasibility and throughput improvement. To realize this, we propose an integrated architecture and formulate a multiobjective optimization problem with mixed integer variables for the joint power control, base station assignment, and channel assignment scheme. In order to find a pareto optimal solution, a weighted sum approach was used. Based on numerical results, the optimization framework is found to be both stable and converging. Simulation studies further show that the proposed architecture and optimization framework improve the aggregate throughput as the client population rises, hence confirming the successful and beneficial integration of these technologies.

1. Introduction

Regulatory bodies throughout the world have found that communication bandwidth is becoming scarce, with two of the major causes being inefficient use of the spectrum and ineffective interference mitigation [1]. Studies have found that the majority of the spectrum bands, particularly the licensed bands, are inefficiently utilized. For example, cellular and ISM bands are overloaded in most parts of the world while UHF TV and amateur radio bands are underutilized in some locations at some specific time instances [2, 3]. In accordance with this, increasing interference levels in the overloaded spectrum render interference mitigation schemes ineffective. In the ISM band, for instance, Bluetooth transmissions suffer from significant packet loss in the presence of WLAN interference [4]. In this work, we make use of cognitive radio and femtocell technology to resolve inefficient spectrum utilization and high levels of interference, respectively.

Cognitive radio (CR) was proposed in an endeavor to allow opportunistic use of unutilized licensed resources, also called spectrum holes, by sensing the communication environment [5]. The sensed information is used to change the communication parameters of cognitive radio users, called *secondary users*, using software-defined radios without producing significant interference to licensed users, called *primary users*. Cognitive radios also exhibit autoconfiguration and intelligent sensing characteristics [6, 7]. On the other hand, femtocells are short-range, low-power base stations installed by customers to limit interference, thereby increasing network capacity, in a small area. The installed device, called a *Femtocell Base Station* (*FBS*), communicates with the main base station, called a *Macrocell Base Station* (*MBS*), either by dedicated channels or wired

communication. The noise mitigation characteristic of the femtocell architecture is a result of "microization", a recent network concept in which a large area network is divided into smaller networks, thereby reducing the per base station load [8].

However, the aforementioned benefits derived from cognitive radios and femtocells may be nonexistent, if not minimal, when implemented separately, due to their respective limitations. In the case of cognitive radio, the spectrum management mechanism of this technology is limited by the user density as well as the communication behavior of primary clients [7]. Contention for spectrum holes also exists due to the large number of secondary clients searching for spectrum holes. In addition, if the utilization of licensed bands is high, the amount of usable bandwidth decreases exponentially as the number of secondary users increases. In contrast, femtocell performance is dependent on the available bandwidth, since the FBSs operate under the same spectrum as MBSs [9]. Upon these considerations, interference mitigation and interference control schemes need to be studied in order to improve cognitive radio performance. In a similar manner, spectrum management schemes should be considered for femtocell implementations. Based on this argument, the integration of cognitive radio and femtocell is expected to be mutually beneficial for these technologies. In addition, we introduce a compensation concept to address the backhaul communication issue for open access femtocells given in [8].

The main contributions of this paper can be summarized as follows.

(i) We propose a system architecture for a cognitive femtocell network architecture that incorporates cognitive radio and femtocells (Section 2).

(ii) We propose a joint power control, base station assignment, and channel assignment scheme for cognitive femtocell networks. In this scheme, the power of each node, as well as the selection of the base station to which a node connects, is controlled so as to maximize the aggregate throughput. In addition, we also propose a compensation scheme to compensate femtocell owners for usage of their resources. We also formulated a mixed integer multiobjective optimization model for the proposed schemes and found the global solution using the branch and bound method (Section 3).

(iii) Finally, we provided numerical and simulation results to show that the proposed joint power control, base station assignment, and channel assignment scheme for cognitive femtocell networks achieves better performance than conventional architectures (Section 4).

2. Problem Definition and System Architecture

We begin by discussing the benefits derived from cognitive radio and how the femtocell architecture gains from the use of CRs. To help with the discussion, graphical representations

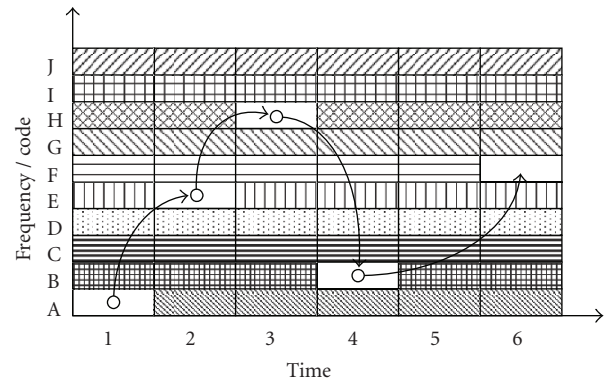

Figure 1: Cognitive Radio Operation. The arrows show the movement of secondary clients from one spectrum hole to another. A spectrum hole is used to describe unused spectrum resource. The vertical axis represents the unit of spectrum resource. For WiMAX and LTE, spectrum resource is classified by frequency while for W-CDMA(UMTS), the spectrum is classified by code.

are presented in Figures 1 and 2. Figure 1 presents a pictorial representation of spectrum mobility, where secondary users transfer to available spectrum, called *spectrum holes*, when the primary users need to use the spectrum currently used by these secondary users. A spectrum hole is a term describing spectrum resources that are unused. Also, for overlay implementations, a spectrum hole is also used to denote a unit of spectrum resource whose Signal to Interference and Noise Ratio (SINR) is below a predefined threshold. Note that *primary users* are those users that own the spectrum/resource while *secondary users* are those users that are opportunistically using the spectrum/resource owned by primary users. In this paper, the MBS is the primary user and each FBS is a secondary users. In Figure 1, there are 10 units of available spectrum resources (A to J) for a particular cell. These units of spectrum resource can be described by frequency bandwidth (WiMAX, LTE) or code assignment (W-CDMA). At time instance 1, an FBS is using resource A. Upon time instance 2, resource A is needed by the MBS, and the FBS needs to find a new spectrum, designated in figure as resource E. A similar event happens in time instance 3 where the FBS releases resource E to continue transmission using resource H. Suppose there are several spectrum holes available, as in time instance 4. In this case, the FBS chooses the spectrum hole that would provide higher throughput, which in Figure 1 is resource B. Furthermore, there is a possibility that no unused resource is available. In this case, as in time instance 5, the FBS may adjust its power and continue using resource B under the condition that it does not add significant interference to the MBS. The FBS continues to transmit in low-power until it finds a new spectrum hole. However, note that if the FBS contributes a significant amount of interference to the macrocell network despite low-power transmission, then the femtocell should defer its transmission until it finds a new spectrum hole. In addition, in a case where several FBSs and a single spectrum hole exist, the FBSs would contend to use the resource. As can be seen in the scenario from Figure 1, the use of

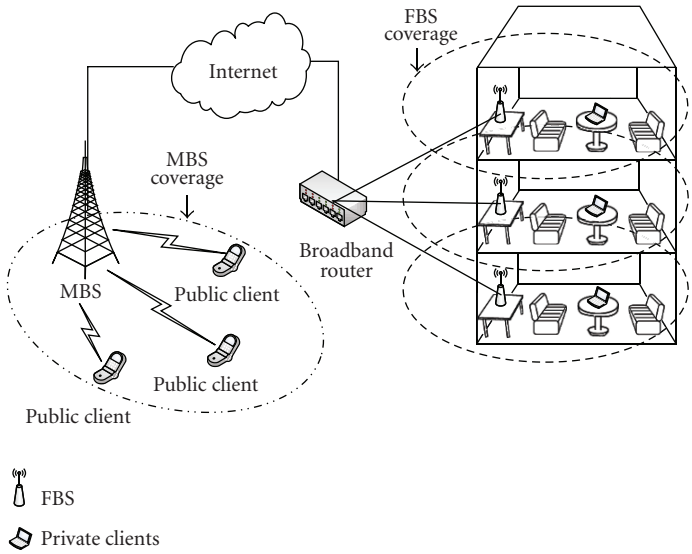

Figure 2: Femtocell Operation. The femtocell architecture consists of several private base stations called FBSs, which service *private clients* who own these FBSs. A main base station called MBS also exists to provide service to nonfemtocell owners, called *public clients.*

cognitive radio exploits sensing the environment to maintain a predetermined threshold of SINR level.

A common femtocell architecture is illustrated in Figure 2. The FBS in this figure communicates with the MBS through the Internet while other means, such as dedicated wireless channels, can be used for connectivity. Coverage enhancement and interference mitigation are two advantages derived from using the femtocell architecture. System coverage is extended since unreachable users can connect to the MBS through the FBSs. On the other hand, FBS installations can also reduce interference in highly dense areas, since private clients do not have to compete for the macrocell network resources [8]. However, different installations of FBSs may interfere with each other, since these base stations usually reuse the same set of frequencies. In a worst-case scenario, such as the apartment setup in Figure 2, massive contention may occur. From this, we can see that the performance of femtocell architectures is limited by the available frequency spectrum [8]. The femtocell architecture benefits from using cognitive radio in that it gains the capability of sensing its environment and can thereupon adapt its configuration based on the sensed information.

With the knowledge of the benefits and limitations of cognitive radio and femtocell technologies, it is straightforward that merging these technologies provides a potential direction to achieve maximum performance. Figure 3 illustrates the architecture proposed in this paper. The system is composed of three major entities: (1) MBS, (2) FBSs, and (3) private and public clients.

The MBS is the central entity of the whole system. As previously mentioned, this base station serves as the primary user of the licensed spectrum and is operated by the service providers. The FBSs are equipped with cognitive radio with spectrum sensing, spectrum management, spectrum sharing,

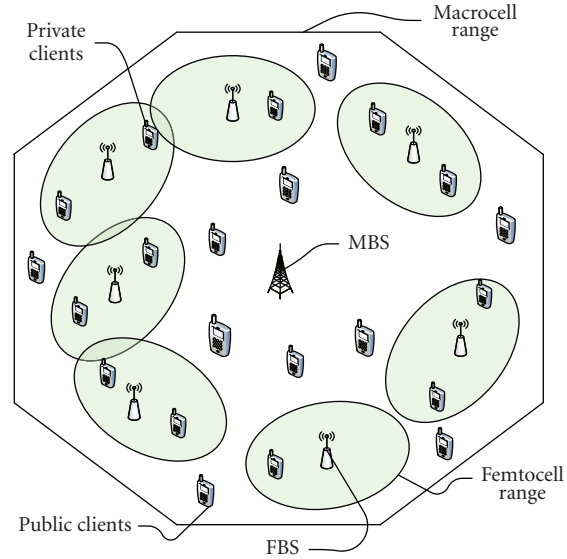

Figure 3: Cognitive femtocell network architecture. The architecture is composed of a single MBS with several FBSs Each FBS controls its power to reduce interference caused to neighbour FBSs and also to the MBS.

and spectrum mobility functionalities, as defined in [7]. With this feature, each FBS has the ability to sense its environment and change to different channels based on the sensed information. Each FBS connects to the MBS via TDMA slotted communication. Each FBS is given time slots used to forward data to the macrocell network.

In addition, we consider an open access femtocell architecture [8]. In this architecture, femtocells allow connection of public clients in order for these clients to connect to

the macrocell network. To support an open access femtocell architecture, a compensation scheme is needed, since the use of an open access femtocell architecture would decrease the effective throughput of private clients. Public clients normally associate with the MBS. In our open access scheme, these public clients may connect to other FBSs under the condition that the FBSs to which these clients connect must be compensated by the MBS. In this paper, these FBSs that accommodate public clients are compensated by being provided additional time slots in backhaul communication. Details of this compensation scheme are given in Section 3. Furthermore, the FBSs may also adjust their power to control their transmission range communication if the MBS requests coverage enhancement and for interference mitigation purposes.

In this paper, we assume that the MBS and FBS use OFDMA-based WiMAX and that resources are assigned based on a frequency-time basis. In addition, each base station is equipped with a single radio and can operate at a single frequency for each time instance. Also, for analysis purposes, its assumed that the cell is on a high-density area and that all clients need to transmit some data.

The problem this paper aims to resolve is the maximization of throughput performance by controlling the BS assignment of public clients, the channel allocation for each BS, and the transmission power. In controlling the power and channel allocation, the interference between clients and BSs is reduced. The BS assignment allows public clients to connect to FBSs subject to compensation from the MBS.

3. Joint Power Control, Base Station Assignment, and Channel Assignment Model

In this paper's model, two objectives are considered. The first objective is to maximize the achievable throughput in the network while the second deals with what we call femtocell compensation. The goal of the whole formulation is to maximize the achievable throughput of the system while minimizing the need for femtocell compensation. In the following subsections, the formulation for uplink and downlink scenarios, as well as the branch and bound method used to solve the scheme, is detailed.

3.1. Uplink Optimization Model. Suppose that a cell consists of 1 MBS, M FBSs, and N client nodes. Also, assume that the cell is provided with J available frequencies. It can be shown that the transmission power of any node i can be expressed in terms of the measured power at any node k, as given by (1). Note that, given that $h^j_{i,i} = 1$, it can be shown that $p_i = \hat{p}^j_{i,i}$. From the Shannon Formula [10], $v^j_{i,k}$ can be formulated as (2). It can be shown that the aggregate uplink achievable throughput can be formulated using (2), as in (3), where $a_i, b_{i,k}$, and $c_{i,k}$ are binary elements of coverage matrices $(\mathbf{A}, \mathbf{B}, \mathbf{C})$, as defined in Table 1. This aggregate uplink achievable throughput $\mathbb{T}^U(\mathbf{A}, \mathbf{C}, \mathbf{F}^U, \mathbf{P})$ is the equation for the first objective of the uplink optimization formulation

$$p_i = \frac{\hat{p}^j_{i,k}}{h^j_{i+M,k}}, \tag{1}$$

$$v^j_{i,k} = \log_2\left(1 + \frac{p_i h^j_{i+M,k}}{\sum_{u\neq i,\, u\in[1,N]} \hat{p}^j_{u,i} h^j_{u+M,k}/h^j_{u+M,i+M} + \mathbb{I}_{\text{noise}}}\right), \tag{2}$$

$$\mathbb{T}^U\left(\mathbf{A}, \mathbf{C}, \mathbf{F}^U, \mathbf{P}\right) : \sum_{j=1}^{J}\sum_{i=1}^{N} a_i f^U_{i,j} v^j_{i,0} + \sum_{j=1}^{J}\sum_{k=1}^{M}\sum_{i=1}^{N} (b_{i,k}+c_{i,k}) f^U_{i,j} v^j_{i,k}. \tag{3}$$

As can be seen from (3), the first objective function for throughout maximization is a joint scheme for incorporating power control, BS assignment, and channel assignment. In this objective function, the power control scheme controls the transmission powers $(\mathbf{P})$ of client nodes in order to minimize the contributed interference. In addition, we define BS assignment $(\mathbf{A}, \mathbf{B}, \mathbf{C})$ as a representation of the BS to which these clients connect, that is, if they are connected to any FBSs or the MBS. The association of public clients to the FBSs is subject to the MBS load and interference conditions. Finally, the channel assignment $(\mathbf{F}^U)$ is chosen from the J available channels for each node. These parameters are computed for each time frame.

Due to the use of an open access femtocell architecture, it is necessary to introduce a scheme to control the backhaul, that is, the communication between MBS and FBSs. For this paper, we assume that a TDMA scheme is used for backhaul communication between MBS and FBSs. Here a fixed time frame τ is initially divided into M slots. Each of the M FBSs gets a dedicated β_{rate}/M data rate for each time slot. In the event that a public client connects to a FBS, the FBS is compensated by getting additional slots in the backhaul. Since our architecture allows public clients to use the FBS, it would incur costs for private clients who own the FBS. These costs shouldered by the private users should be compensated by the service providers of the macrocell network. In order to quantify the amount of backhaul bandwidth used by public clients, the achievable uplink throughput value of the public client and aggregate uplink throughput value at the FBS are compared, as seen in (4). $\mathbb{C}^U(\mathbf{C}, \mathbf{F}^U, \mathbf{P})$ quantifies the bandwidth lost by the private clients and used by the public clients. The compensation mechanism in (4) provides the FBS with a means to increase backhaul traffic rate as compensation for the decreased data transmission rate in the uplink towards the FBS:

$$\mathbb{C}^U\left(\mathbf{C}, \mathbf{F}^U, \mathbf{P}\right) = \sum_{k=1}^{M} \frac{\beta_{\text{rate}} \dfrac{\sum_{j=1}^{J}\sum_{i=1}^{N} (c_{i,k}) f^U_{i,j} v^j_{i,k}}{\sum_{j=1}^{J}\sum_{i=1}^{N} (b_{i,k}+c_{i,k}) f^U_{i,j} v^j_{i,k}}}{M + \dfrac{\sum_{j=1}^{J}\sum_{i=k}^{K} (c_{i,k}) f^U_{i,j} v^j_{i,k}}{\sum_{j=1}^{J}\sum_{i=1}^{N} (b_{i,k}+c_{i,k}) f^U_{i,j} v^j_{i,k}}}. \tag{4}$$

Table 1: Notation summary.

Symbol	Description
M	Total number of FBS
N	Total number of clients
$\mathbb{I}_{\text{noise}}$	Hardware noise and environmental noise
τ	Time frame
β_{rate}	Maximum backhaul link capacity
$\gamma_{\text{th}}^{\text{PU}}$	Constant parameter for the SINR threshold of MBS
$\gamma_{\text{th}}^{\text{SU}}$	Constant parameter for the SINR threshold of the FBS
P_{MAX}	Constant parameter for the maximum transmission power of clients
$Q_{\text{MAX}}^{\text{MBS}}$	Constant parameter for the maximum transmission power of MBS
$Q_{\text{MAX}}^{\text{FBS}}$	Constant parameter for the maximum transmission power of FBS
w	Weight parameter for the weighted sum approach
$\mathbf{P} = \{p_i \mid i = \overline{1,N}\}$	Transmission power vector of clients
$\mathbf{Q} = \{q_k \mid k = \overline{0,M}\}$	Transmission power vector of BS
$\hat{\mathbf{P}} = \{\hat{p}_{i,k}^j \mid i,k = \overline{1,N}, j = \overline{1,J}\}$	Measured power of client k at client i using channel j
$\mathbf{Q} = \{\hat{q}_{i,k}^j \mid i,k = \overline{0,M}, j = \overline{1,J}\}$	Measured power of BS k at BS i
$v_{i,k}^j$	Uplink achievable throughput from client i to BS k using frequency j
$\delta_{k,i}^j$	Downlink achievable throughput from BS k to client i using frequency j
$\mathbf{H} = \{h_{i,k}^j \mid h_{i,i}^j = 1, h_{i,k}^j = h_{k,i}^j,$ $i = \overline{0,N+M+1}, k = \overline{0,N+M+1}, j = \overline{1,J}\}$	Transmission gain matrix between network elements. Note that index 0 represents the MBS, indices 1 to M represent FBSs, and indices $M+1$ to $M+N$ represent clients
$\mathbf{A} = \{a_i \mid i = \overline{1,N}\}$	Coverage scheme variable for set of public users associated with MBS
$\mathbf{B} = \{b_{i,k} \mid i = \overline{1,N}, k = \overline{1,M}\}$	Coverage scheme constant for set of private users i associated with an FBS k
$\mathbf{C} = \{c_{i,k} \mid i = \overline{1,N}, k = \overline{1,M}\}$	Coverage scheme variable for set of public users i associated with FBS k
$\mathbf{F}^U = \{f_{i,j}^U \mid i = \overline{1,N}, j = \overline{1,J}\}$	Uplink channel assignment variable for client i using frequency j
$\mathbf{F}^D = \{f_{k,j}^D \mid k = \overline{0,N}, j = \overline{1,J}\}$	Downlink channel assignment variable for BS k using frequency j
$\mathbb{T}^U(\mathbf{A}, \mathbf{C}, \mathbf{F}^U, \mathbf{P})$	Uplink throughput objective function
$\mathbb{T}_i^U(a_i, \mathbf{C}_i, \mathbf{F}_i^U, p_i)$	Distributed uplink throughput objective function at each client i
$\mathbb{T}^D(\mathbf{A}, \mathbf{C}, \mathbf{F}^D, \mathbf{Q})$	Downlink throughput objective function
$\mathbb{T}_0^D(\mathbf{F}_0^D, q_i)$	Distributed downlink throughput for the MBS
$\mathbb{T}_k^D(\mathbf{F}_k^D, q_i)$	Distributed downlink throughput at each FBS
$\mathbb{C}^U(\mathbf{C}, \mathbf{F}^U, \mathbf{P})$	Uplink compensation objective function
$\mathbb{C}^D(\mathbf{C}, \mathbf{F}^D, \mathbf{Q})$	Downlink compensation objective function
$\mathbb{C}_i^U(\mathbf{C}_i, \mathbf{F}_i^U, p_i)$	Distributed compensation objective function at each client i
$\mathbb{C}_k^D(\mathbf{F}_k^D, q_k)$	Distributed downlink compensation objective function at each BS k
$W^U(\mathbf{A}, \mathbf{C}, \mathbf{F}^U, \mathbf{P})$	Weighted sum problem for uplink model
$W_i^U(a_i, \mathbf{C}_i, \mathbf{F}_i^U, p_i)$	Distributed uplink weighted sum problem
$W^D(\mathbf{A}, \mathbf{C}, \mathbf{F}^D, \mathbf{Q})$	Weighted sum problem for downlink model
$W_0^D(\mathbf{F}_0^D, q_0)$	Distributed downlink weighted sum problem at the MBS
$W_k^D(\mathbf{F}_k^D, q_k)$	Distributed downlink weighted sum problem at each FBS
$v_{e-i,k}^j$	Distributed achievable throughput from client i to BS k using frequency j at each client e
$\delta_{e-k,i}^j$	Downlink achievable throughput from BS k to client i using frequency j at each BS e

We illustrate this using Figure 2. Suppose a private client at the first floor of the apartment is connected to the FBS that he/she owns. Assume the backhaul link has a link capacity of 1 Mpbs. In the figure, there are a total of 3 FBSs in the network; then each of these FBSs experiences an effective rate of 0.33 Mbps in the backhaul. Now suppose that a public client connects to the FBS at the first floor and the ratio of the achievable uplink throughput of the public client and aggregate uplink throughput at that FBS is 0.15, that is, 15% of the bandwidth are used by the public clients. In this scenario, the backhaul capacity is divided into 3.15. The first floor FBS that connects the public client gets a 0.37 Mbps

effective backhaul rate while the other 2 FBSs in the second and third floors receive 0.317 Mbps:

$$\max_{(\mathbf{A},\mathbf{C},\mathbf{F}^U,\mathbf{P})} \mathbb{T}^U\left(\mathbf{A},\mathbf{C},\mathbf{F}^U,\mathbf{P}\right), \tag{5a}$$

$$\min_{(\mathbf{C},\mathbf{F}^U,\mathbf{P})} \mathbb{C}^U\left(\mathbf{C},\mathbf{F}^U,\mathbf{P}\right), \tag{5b}$$

$$\text{such that } a_i + \sum_{k=1}^{M}\left(b_{i,k}+c_{i,k}\right) = 1, \tag{5c}$$

$$\frac{a_i p_i h_{i+M,0}^j}{\sum_{u\neq i,\, u\in[1,N]} \widehat{p}_{u,i}^j h_{u+M,0}^j / h_{u+M,i+M}^j + \mathbb{I}_{\text{noise}}} \geq \gamma_{\text{th}}^{\text{PU}}, \tag{5d}$$

$$\frac{\left(b_{i,k}+c_{i,k}\right) p_i h_{i+M,k}^j}{\sum_{u\neq i,\, u\in[1,N]} \widehat{p}_{u,i}^j h_{u+M,k}^j / h_{u+M,i+M}^j + \mathbb{I}_{\text{noise}}} \geq \gamma_{\text{th}}^{\text{SU}}, \tag{5e}$$

$$\sum_{j=1}^{J} f_{i,j}^U \leq 1, \quad i = 1,2,\ldots,N, \tag{5f}$$

$$0 \leq p_i \leq P_{\text{MAX}}, \quad i = 1,2,\ldots,K,$$

$$a_i, c_{i,k}, f_{i,j}^U \in \{0,1\}, \tag{5g}$$

$$i = 1,2,\ldots,K,\ k = 1,2,\ldots,M.$$

The multiobjective problem is formulated in (5a) to (5g). The first objective (5a) maximizes the aggregate uplink throughput given by (3). The second objective (5b) minimizes the compensation objective given by (4). Note that the compensation objective $\mathbb{C}^U(\mathbf{C},\mathbf{F}^U,\mathbf{P})$ is minimized, since the ideal case is for public users to connect using the MBS. Also, an increase in the compensation for a certain FBS would result in a decrease in the backhaul rate for other FBSs. There are five major constraints for the formulation in (5a) to (5g). The first constraint (5c) assures that sets **A**, **B**, or **C** are disjoint. Moreover, this implies that each client associates with only one base station. The next two constraints, given by (5d) and (5e), denote the SINR constraints for each base station. The constraint in (5f) states that a client or FBS is assigned only one frequency. Finally, (5g) describes the limit in transmission power for each client in the uplink.

The multiobjective problem is solved jointly using a weighted-sum approach with the objective function given by (6a) to (6g). In order to incorporate the two objectives, a weight parameter w is introduced. The value of the parameter is limited by (6g). The optimal value of the weight is determined by finding the pareto optimal solution for the two objective functions, $\mathbb{T}^U(\mathbf{A},\mathbf{C},\mathbf{F}^U,\mathbf{P})$ and $\mathbb{C}^U(\mathbf{C},\mathbf{F}^U,\mathbf{P})$:

$$W^U\left(\mathbf{A},\mathbf{C},\mathbf{F}^U,\mathbf{P}\right):$$

$$\max_{(\mathbf{A},\mathbf{C},\mathbf{F}^U,\mathbf{P})} w\mathbb{T}^U\left(\mathbf{A},\mathbf{C},\mathbf{F}^U,\mathbf{P}\right) - (1-w)\mathbb{C}^U\left(\mathbf{C},\mathbf{F}^U,\mathbf{P}\right) \tag{6a}$$

$$\text{such that } a_i + \sum_{k=1}^{M}\left(b_{i,k}+c_{i,k}\right) = 1, \tag{6b}$$

$$\frac{a_i p_i h_{i+M,0}^j}{\sum_{u\neq i,\, u\in[1,N]} \widehat{p}_{u,i}^j h_{u+M,0}^j / h_{u+M,i+M}^j + \mathbb{I}_{\text{noise}}} \geq \gamma_{\text{th}}^{\text{PU}}, \tag{6c}$$

$$\frac{\left(b_{i,k}+c_{i,k}\right) p_i h_{i+M,k}^j}{\sum_{u\neq i,\, u\in[1,N]} \widehat{p}_{u,i}^j h_{u+M,k}^j / h_{u+M,i+M}^j + \mathbb{I}_{\text{noise}}} \geq \gamma_{\text{th}}^{\text{SU}}, \tag{6d}$$

$$\sum_{j=1}^{J} f_{i,j}^U \leq 1, \quad i = 1,2,\ldots,N, \tag{6e}$$

$$0 \leq p_i \leq P_{\text{MAX}}, \quad i = 1,2,\ldots,K, \tag{6f}$$

$$0 < w < 1,$$

$$a_i, c_{i,k}, f_{i,j}^U \in \{0,1\}, \tag{6g}$$

$$i = 1,2,\ldots,N,\ k = 0,1,2,\ldots,M.$$

3.2. Downlink Optimization Model. It has been shown [11] that the uplink and downlink models for general wireless networks can be formulated through duality by changing constraints under the assumption that the transmission gain matrix is symmetric, that is, $h_{i,k}^j = h_{k,i}^j$. Based on this principle, we can formulate the downlink model as follows. The downlink achievable throughput is defined as in (7). For the downlink transmission, the aggregate throughput and compensation objective functions can be derived, as given in (8) and (9), respectively,

$$\delta_{k,i}^j = \log\left(1 + \frac{q_k h_{k,i+M}^j}{\sum_{u\neq k,\, u\in[0,M]} \widehat{q}_{u,k}^j h_{u,i+M}^j / h_{u,k}^j + \mathbb{I}_{\text{noise}}}\right), \tag{7}$$

$$\mathbb{T}^D(\mathbf{A},\mathbf{C},\mathbf{F}^D,\mathbf{Q}) : \sum_{j=1}^{J}\sum_{i=1}^{N} a_i f_{i,j}^D \delta_{0,i}^j + \sum_{j=1}^{J}\sum_{k=1}^{M}\sum_{i=1}^{N}\left(b_{i,k}+c_{i,k}\right) f_{i,j}^D \delta_{k,i}^j, \tag{8}$$

$$\mathbb{C}^D\left(\mathbf{C},\mathbf{F}^D,\mathbf{Q}\right) = \sum_{k=1}^{M} \frac{\beta_{\text{rate}} \dfrac{\sum_{j=1}^{J}\sum_{i=1}^{N}\left(c_{i,k}\right) f_{i,j}^D \delta_{k,i}^j}{\sum_{j=1}^{J}\sum_{i=1}^{N}\left(b_{it}+c_{it}\right) f_{i,j}^D \delta_{k,i}^j}}{M + \dfrac{\sum_{j=1}^{J}\sum_{i=1}^{N}\left(c_{i,k}\right) f_{i,j}^D \delta_{k,i}^j}{\sum_{j=1}^{J}\sum_{i=1}^{N}\left(b_{i,k}+c_{i,k}\right) f_{i,j}^D \delta_{k,i}^j}}. \tag{9}$$

In a similar manner, the downlink optimization model can be formulated as in (10a) to (10h). It can be observed that the duality formulation differs only in the transmission power vector Q and the transmission gain matrix. However, considering the assumption that the transmission gain matrix is symmetric, then the formulation is similar to the

(1) BEGIN
(2) Initialize. $CURR = \infty$, $LB(S_0) = G(S_0)$, $LIVESET = S_0$, $count = 0$
(3) Get Problem from $LIVESET$; $S_{\text{PARENT}} = LIVESET(count)$
(4) **while** $LIVESET \neq \phi$ **do**
(5) Branch out sets from S_A and S_B from S_{PARENT} such that $S_A \cup S_B = S_{\text{PARENT}}$
(6) Prune S_{PARENT}; $count = count - 1$
(7) Compute $LB(S_A) = G(S_A)$, $LB(S_B) = G(S_B)$
(8) **if** $LB(S_A) > LB(S_B)$ **then**
(9) Append S_A to $LIVESET$; $count = count + 1$
(10) Append S_B to $LIVESET$; $count = count + 1$
(11) **else**
(12) Append S_B to $LIVESET$; $count = count + 1$
(13) Append S_A to $LIVESET$; $count = count + 1$
(14) **end if**
(15) Get Problem from $LIVESET$; $S_{\text{PARENT}} = LIVESET(count)$
(16) **if** $LB(S_{\text{PARENT}}) = F(\widetilde{A}, \widetilde{C}, \widetilde{F}, \widetilde{P})$ for a feasible solution $(\widetilde{A}, \widetilde{C}, \widetilde{F}, \widetilde{P})$ **then**
(17) **if** $F(\widetilde{X}) < CURR$ **then**
(18) $CURR = F(\widetilde{A}, \widetilde{C}, \widetilde{F}, \widetilde{P})$; $(\widetilde{A}^*, \widetilde{C}^*, \widetilde{F}^*, \widetilde{P}^*) = (\widetilde{A}, \widetilde{C}, \widetilde{F}, \widetilde{P})$
(19) **end if**
(20) **end if**
(21) **if** $LB(S_{\text{PARENT}}) \geq CURR$ **then**
(22) Prune S_{PARENT} from $LIVESET$; $count = count - 1$
(23) Get Problem from $LIVESET$; $S_{\text{PARENT}} = LIVESET(count)$
(24) **end if**
(25) **end while**
(26) END.

Algorithm 1: Branch and bound method.

uplink model:

$$W^D\left(\mathbf{A}, \mathbf{C}, \mathbf{F}^D, \mathbf{Q}\right): \max_{(\mathbf{A},\mathbf{C},\mathbf{F}^D,\mathbf{Q})} w\mathbb{T}^D\left(\mathbf{A}, \mathbf{C}, \mathbf{F}^D, \mathbf{Q}\right) - (1-w)\mathbb{C}^D\left(\mathbf{C}, \mathbf{F}^D, \mathbf{Q}\right) \tag{10a}$$

$$\text{such that } a_i + \sum_{k=1}^{M}\left(b_{i,k} + c_{i,k}\right) = 1, \tag{10b}$$

$$\frac{a_i q_0 h^j_{0,i+M}}{\sum_{u\neq 0,\, u\in[0,M]} \hat{q}^j_{u,0} h^j_{u,i+M}/h^j_{u,0} + \mathbb{I}_{\text{noise}}} \geq \gamma^{\text{PU}}_{\text{th}}, \tag{10c}$$

$$\frac{(b_{i,k} + c_{i,k}) q_k h^j_{k,i+M}}{\sum_{u\neq k,\, u\in[0,M]} \hat{q}^j_{u,k} h^j_{u,i+M}/h^j_{u,k} + \mathbb{I}_{noise}} \geq \gamma^{\text{SU}}_{\text{th}}, \tag{10d}$$

$$\sum_{j=1}^{J} f^D_{i,j} \leq 1, \quad i = 1, 2, \ldots, N, \tag{10e}$$

$$0 \leq q_0 \leq Q^{\text{MBS}}_{\text{MAX}}, \tag{10f}$$

$$0 \leq q_k \leq Q^{\text{FBS}}_{\text{MAX}}, \quad k = 1, 2, \ldots, K, \tag{10g}$$

$$0 < w < 1,$$

$$a_i, c_{i,k}, f^D_{i,j} \in \{0, 1\}, \tag{10h}$$

$$i = 1, 2, \ldots, N,\ k = 0, 1, 2, \ldots, M.$$

3.3. Joint Power Control, Base Station Assignment, and Channel Assignment Scheme using Branch and Bound Method. It can be shown that the uplink and downlink joint power control, base station assignment, and channel assignment scheme formulation problems in (6a) to (6g) and (10a) to (10h) are nonconvex problems due to the mixed integer problem and high-order objectives. These types of problems are well-known NP-Hard problems. However, for a fixed number of variables, the branch and bound method is capable of solving a mixed integer problem in predetermined time. The branch and bound method used in this paper is given by Algorithm 1. The notation for parameters used in the method are provided in Table 2. The method begins by initializing the parameters needed for the method (line 2). The *CURR* parameter represents the upper bound of the solution. The branch and bound method starts from an initial set S_0, which is listed in the set list *LIVESET*. In this case, S_0 is the set of possible solutions for the uplink and downlink problems without the constraint $a_i, c_{i,k}, f^U_{i,j} \in \{0, 1\}$, that is, the integer variables are relaxed and considered to be continuous variables. The lower bound for set S_0 can be found by solving the problem using convex problem methods. In this paper, we used the conditional gradient method [12], represented by the function $G(S)$, where S is the current set analyzed. Then, while *LIVESET* is not empty, the method performs (line 5) to (line 25).

We take a set S_{PARENT} from *LIVESET* and branch out to two sets, S_A and S_B, where $S_A \bigcup S_B = S_{\text{PARENT}}$ (line 5). S_{PARENT} is then pruned from *LIVESET*, since it has already

Table 2: Branch and bound method notation summary.

Symbol	Meaning
CURR	Current upper bound
$LB(S)$	Lower bound of the problem on set S
$G(S)$	Conditional gradient method over set S
LIVESET	Set of unanalyzed sets
S_A, S_B	Offspring set of each iteration
S_{PARENT}	Current iteration's parent set

produced all its offspring (line 6). After pruning S_{PARENT}, the method decides the order in which S_A and S_B should be inserted into *LIVESET* (line 7–line 14). To determine the order, the value of the lower bound for each of S_A and S_B is computed. The set whose lower bound is lower is analyzed first. These series of steps are important, because if a solution is found traversing the set a lesser lower bound, then the likelihood of finding a better solution from the other set would be decreased. The set with a lesser lower bound is chosen as S_{PARENT} (line 15). A check procedure is conducted if the $LB(S_{\text{PARENT}})$ is a feasible solution for the unrelaxed problems in (6a) to (6g) and (10a) to (10h). If this is true, then the upper bound *CURR* is adjusted to $LB(S_{\text{PARENT}})$ and the current solution is $(\widetilde{A}, \widetilde{C}, \widetilde{F}, \widetilde{P})$ (line 16–line 21). Another check is conducted if the lower bound of S_{PARENT} is greater than the upper bound *CURR*, and then no better solution can be found inside the set S_{PARENT}. S_{PARENT} is then pruned from *LIVESET* and the next parent is taken from *LIVESET* (line 21–24). If both conditions in line 16 and line 21 are not met, then the method branches out and prunes the current S_{PARENT}. The process repeats until *LIVESET* is empty.

The method presented in Algorithm 1 is a First-In Last-Out search technique applied to the branch and bound method. As mentioned previously, analyzing sets whose lower bounds are lesser than other sets reduces the probability of the need to analyze the other sets. As such, the computation time can be proven to be between $\mathbb{O}(N)$ and $\mathbb{O}(2^{N-1})$.

3.4. Distributed Implementation of the Joint Power Control, Base Station Assignment, and Channel Assignment Scheme. To implement the Joint power control, base station assignment and channel assignment scheme in a distributed way, we first look at the separability of the objective functions in (6a) to (6g) and (10a) to (10h) and, as well as the separability of the constraint set:

$$\mathbb{T}_i^U\left(a_i, \mathbf{C}_i, \mathbf{F}_i^U, p_i\right) : \sum_{j=1}^{J} a_i f_{i,j}^U v_{i,0}^j + \sum_{j=1}^{J}\sum_{k=1}^{M} (b_{i,k} + c_{i,k}) f_{i,j}^U v_{i,k}^j, \tag{11}$$

$$v_{-ei,k}^j = \log_2\left(1 + \frac{\widehat{p}_{i,e}^j h_{i+M,k}^j / h_{i+M,e+M}^j}{\sum_{u\neq eu\in[1,N]} \widehat{p}_{u,i}^j h_{u+M,k}^j / h_{u+M,i+M}^j + \mathbb{I}_{\text{noise}}}\right), \tag{12}$$

$$\mathbb{C}_i^U\left(\mathbf{C}_i, \mathbf{F}_i^U, p_i\right) = \sum_{k=1}^{M} \frac{\beta_{\text{rate}}\varphi}{M+\varphi}, \tag{13}$$

where

$$\varphi = \frac{\sum_{j=1}^{J}\sum_{e=1}^{N} (c_{i,k}) f_{i,j}^U v_{-ei,k}^j}{\sum_{j=1}^{J}\sum_{e=1}^{N} (b_{ek} + c_{ek}) f_e^j v_{-ie,k}^j}. \tag{14}$$

For the objective function, the throughput objective for the uplink joint power control, base station assignment, and channel assignment scheme (3) is observed to be separable to (11) for each client i. For the compensation mechanism in (4), the nonseparability lies in the sum of achievable throughputs at a BS given by $\sum_{j=1}^{J}\sum_{t=1}^{M}\sum_{i=1}^{K}(b_{i,k}+c_{i,k}) f_{i,j}^U v_{i,k}^j$. To resolve this, the measure power of neighbor nodes and (1) is used to modify (4). Let $v_{ei,k}^j$ (12) be the uplink achievable throughput between client i and BS k as seen from BS e using channel j. Using (12), the compensation mechanism in (4) can be separable as in (13). Finally, it is easily seen that the constraint sets for the uplink joint power control, base station assignment, and channel assignment scheme are separable

$$\begin{aligned}
&W_i^U\left(a_i, \mathbf{C}_i, \mathbf{F}_i^U, p_i\right) :\\
&\max_{(a_i, C_i, F_i^U, p_i)} w\mathbb{T}_i^U\left(a_i, C_i, F_i^U, p_i\right) - (1-w)\mathbb{C}_i^U\left(C_i, F_i^U, p_i\right)\\
&\text{such that } a_i + \sum_{k=1}^{M}(b_{i,k} + c_{i,k}) = 1,\\
&\frac{a_i p_i h_{i+M,0}^j}{\sum_{u\neq i, u\in[1,N]} \widehat{p}_{u,i}^j h_{u+M,k}^j / h_{u+M,i+M}^j + \mathbb{I}_{\text{noise}}} \geq \gamma_{\text{th}}^{\text{PU}},\\
&\frac{(b_{i,k}+c_{i,k}) p_i h_{i+M,k}^j}{\sum_{u\neq i, u\in[1,N]} \widehat{p}_{u,i}^j h_{u+M,k}^j / h_{u+M,i+M}^j + \mathbb{I}_{\text{noise}}} \geq \gamma_{\text{th}}^{\text{SU}},\\
&\sum_{j=1}^{J} f_{i,j}^U \leq 1,\\
&0 \leq p_i \leq P_{\text{MAX}},\\
&0 < w < 1,\\
&a_i, c_{i,k}, f_{i,j}^U \in \{0, 1\}.
\end{aligned} \tag{15}$$

From (11) to (13), the uplink joint power control, base station assignment, and channel assignment scheme in (6a) to (6g) can be reformulated as (15) for each client.

We consider the problem of maximizing the total utility functions over separable sets. It can be shown that the objective function in (15) is nonconvex. The optimal solutions in (15) with separable functions are characterized in Lemma 1. Let

$$\begin{aligned}
&\Phi_i^U\left(\mathbf{A}, \mathbf{C}, \mathbf{F}^U, \mathbf{P}\right)\\
&\quad = w\mathbb{T}_i^U\left(a_i, \mathbf{C}_i, \mathbf{F}_i^U, p_i\right) - (1-w)\mathbb{C}_i^U\left(\mathbf{C}_i, \mathbf{F}_i^U, p_i\right),\\
&\Phi^U\left(\mathbf{A}, \mathbf{C}, \mathbf{F}^U, \mathbf{P}\right) = \sum_{i=1}^{N} \Phi_i^U.
\end{aligned} \tag{16}$$

Lemma 1. *Assume that* $(a_i^*, \mathbf{C}_i^*, \mathbf{F}_i^U *, p_i^*)$, $i = \overrightarrow{1,N}$, *is the solution for* (15) *at each i. Then* $\mathbf{A}^* = (a_1^*, a_2^*, \ldots, a_N^*)$, $\mathbf{C}^* = (\mathbf{C}_1^*, \mathbf{C}_2^*, \ldots, \mathbf{C}_N^*)$, $F^{U*} = (\mathbf{F}_1^{U*}, \mathbf{F}_2^{U*}, \ldots, \mathbf{F}_N^{U*})$, $\mathbf{P}^* = (p_1^*, p^*, \ldots, p_N^*)$.

Proof. The proof is an obvious consequence of the following inequalities:

$$\begin{aligned}
&\Phi^U\left(\mathbf{A}, \mathbf{C}, \mathbf{F}^U, \mathbf{P}\right) \\
&= \sum_{i=1}^{N} \Phi_i^U\left(\mathbf{A}, \mathbf{C}, \mathbf{F}^U, \mathbf{P}\right) \le \sum_{i=1}^{N} W_i^U\left(a_i, \mathbf{C}_i, \mathbf{F}_i^U, p_i\right) \\
&= \sum_{i=1}^{N} \Phi_i^U\left(a_i^*, \mathbf{C}_i^*, \mathbf{F}_i^{U*}, p_i^*\right) = \Phi^U\left(a_i^*, \mathbf{C}_i^*, \mathbf{F}_i^{U*}, p_i^*\right).
\end{aligned} \tag{17}$$

□

The distributed implementation for the downlink joint power control, base station assignment, and channel assignment scheme can be formulated in a similar way as the uplink scheme. In the downlink, we consider the distributed computation by having each BS controls its power, base station assignment, and channel assignment. It is assumed that the uplink solutions for $\mathbf{A}$ and $\mathbf{C}$ are used by the downlink. In this way, the downlink implementation only solves the optimal value for $\mathbf{F}^D$ and $\mathbf{P}$. The throughput can be formulated for MBS and FBSs as (18) and (19), respectively. Let $\delta_{e\leftarrow k,i}^j$ (20) be the uplink achievable throughput between client i and BS k as seen from BS e using channel j:

$$\mathbb{T}_0^D\left(\mathbf{F}_0^D, q_0\right) : \sum_{j=1}^{J} \sum_{i=1}^{N} a_i f_{i,j}^D \delta_{0,i}^j, \tag{18}$$

$$\mathbb{T}_k^D\left(\mathbf{F}_k^D, q_k\right) : \sum_{j=1}^{J} \sum_{i=1}^{N} \left(b_{i,k} + c_{i,k}\right) f_{i,j}^D \delta_{k,i}^j, \tag{19}$$

$$\delta_{ek,i}^j = \log_2\left(1 + \frac{\hat{q}_{i,e}^j h_{k,i+M}^j / h_{i,e}^j}{\sum_{u \ne e,\, u \in [0,M]} \hat{q}_{u,e}^j h_{u,i+M}^j / h_{u,e}^j + \mathbb{I}_{\text{noise}}}\right). \tag{20}$$

From (18) to (20), the compensation mechanism for distributed implementation at each FBS is given as (21). Note that there is no compensation scheme at the MBS:

$$\mathbb{C}_k^D\left(\mathbf{F}_k^D, q_k\right) = \frac{\beta_{\text{rate}} \psi}{M + \psi}, \tag{21}$$

where

$$\psi = \frac{\sum_{j=1}^{J} \sum_{i=1}^{N} \left(c_{i,k}\right) f_{i,j}^D \delta_{e\leftarrow i,k}^j}{\sum_{j=1}^{J} \sum_{i=1}^{N} \left(b_{it} + c_{it}\right) f_{i,j}^D \delta_{e\leftarrow i,k}^j}. \tag{22}$$

The distributed downlink joint power control, base station assignment and channel assignment scheme for MBS and FBS is given by (23) and (24), respectively. It should be pointed out that in (24), the constraint regarding the SINR threshold for the MBS is still included. This is because the FBSs, which are considered secondary users, should use the spectrum with the condition that the SINR of the MBS is not exceeded:

$$\begin{aligned}
&W_0^D\left(\mathbf{F}_0^D, q_0\right) : \\
&\max_{\left(\mathbf{F}_0^D, q_k\right)} \mathbb{T}_0^D\left(a_i, \mathbf{C}_i, \mathbf{F}_0^D, q_i\right) \\
&\text{such that } \frac{a_i q_0 h_{0,i+M}^j}{\sum_{u \ne 0,\, u \in [0,M]} \hat{q}_{u,0}^j h_{0,i+M}^j / h_{u,0}^j + \mathbb{I}_{\text{noise}}} \ge \gamma_{\text{th}}^{\text{PU}}, \\
&\sum_{j=1}^{J} f_{i,j}^D \le 1, \\
&0 \le q_0 \le Q_{\text{MAX}}^{\text{MBS}}, \\
&f_{i,j}^D \in \{0, 1\},
\end{aligned} \tag{23}$$

$$\begin{aligned}
&W_k^D\left(\mathbf{F}_k^D, q_k\right) : \\
&\max_{\left(\mathbf{F}_k^D, q_k\right)} w\mathbb{T}_k^D\left(\mathbf{F}_k^D, q_k\right) - (1 - w)\mathbb{C}_k^D\left(\mathbf{F}_k^D, q_k\right) \\
&\text{such that } \frac{a_i\left(\hat{q}_{0,k}^j h_{0,i+M}^j / h_{0,k}^j\right)}{\sum_{u \ne 0,\, u \in [0,M]} \hat{q}_{u,0}^j h_{0,i+M}^j / h_{u,0}^j + \mathbb{I}_{\text{noise}}} \ge \gamma_{\text{th}}^{\text{PU}}, \\
&\frac{\left(b_{i,k} + c_{i,k}\right) q_k h_{k,i+M}^j}{\sum_{u \ne k,\, u \in [0,M]} \hat{q}_{u,k}^j h_{u,i+M}^j / h_{u,k}^j + \mathbb{I}_{\text{noise}}} \ge \gamma_{\text{th}}^{\text{SU}}, \\
&\sum_{j=1}^{J} f_{i,j}^D \le 1, \\
&0 \le q_k \le Q_{\text{MAX}}^{\text{FBS}}, \\
&0 < w < 1, \\
&f_{i,j}^D \in \{0, 1\}.
\end{aligned} \tag{24}$$

With the formulation for distributed implementation, the overall optimization problem can be solved by each element in the network. Each element computes the solution to the problem by running Algorithm 1 for each of their distributed problems given in (15), (23), and (24).

4. Simulation Studies and Numerical Results

A numerical simulation was conducted to explore the consequences of the formulation and to show that the branch and bound method converges to the optimal solution. The numerical analysis is conducted using MATLAB. The numerical analysis scenario consists of one MBS, three FBSs (FBS_A, FBS_B, and FBS_C), one private client for each FBS (MC_1, MC_2, and MC_3, resp.), and randomly distributed public clients. The SINR threshold for the MBS is set at 0.8 while the SINR threshold for the FBSs is set to 0.3. These high SINR threshold values simulate high-density traffic in the area and assure that the FBSs will have to search for

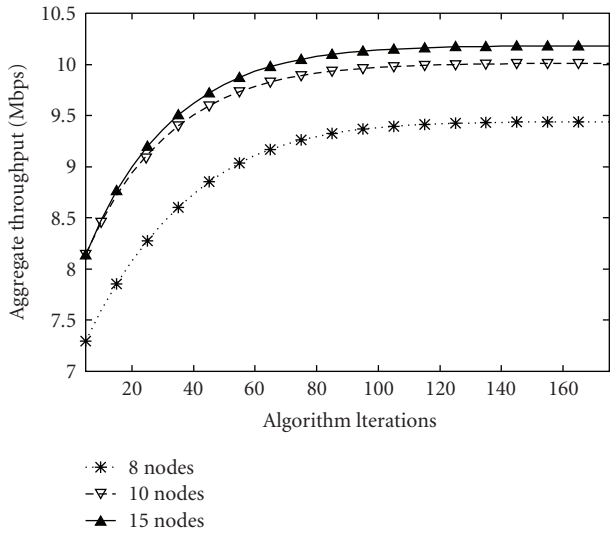

Figure 4: Convergence of the branch and bound method for the joint power control, base station assignment, and channel assignment scheme. The number of nodes is varied from 8,10 and 15 clients. The clients are randomly distributed in each of the 8-client, 10-client, and 15-client configurations except for 3 private clients.

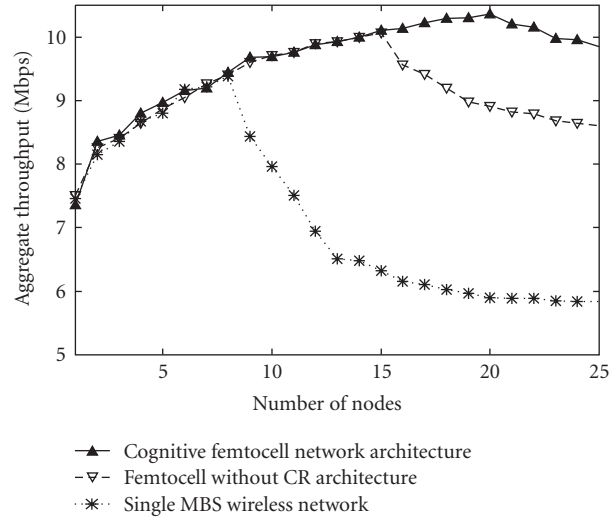

Figure 5: Network achievable throughput. The achievable throughput for our joint power control, base station assignment, and channel assignment scheme is compared with the throughput of Li et al. and a single MBS WiMAX network as the number of nodes is varied.

available spectrum holes. The MBS power $Q_{\text{MAX}}^{\text{MBS}}$ is limited to 1 W while the FBS's power threshold $Q_{\text{MAX}}^{\text{FBS}}$ is at 0.5 W.

The convergence of the conditional gradient method for power optimization can be seen from Figure 4 for 8-node, 10-node, and 15-node configurations. As can be seen in this figure, the solution converges to the optimal solution for a given number of nodes after about 150 iterations. Each iteration involves the splitting of a parent set, as seen in Algorithm 1.

The performance of the architecture is also compared to that of a femtocell network without CR and a traditional single MBS wireless network, respectively. This performance comparison shows the benefits of the cognitive femtocell network architecture in terms of throughput improvement when compared with current architectures. It can be seen from Figure 5 that, as the number of nodes increases, the proposed cognitive femtocell network architecture outperforms both of the traditional networks. The improvement originates from the femtocell owners allowing public clients to utilize their private resources. For less than 8 nodes, the cognitive femtocell behaves in a manner similar to that of a traditional femtocell. In addition, in cases of congestion, the FBS searches for new spectrum holes, which further increases performance. As expected, the performance of the single MBS wireless network degrades as the number of clients increases. In addition, we observe that as the number of clients increases, the macrocell cannot meet the SINR threshold requirement. Thus, some clients are not allowed to transmit. Traditional femtocell networks behave similarly to the cognitive femtocell network architecture. However, when congestion occurs (in this case at $N = 15$), the performance of the traditional femtocell degrades. Upon congestion at $N = 15$, the cognitive femtocell searches for spectrum holes.

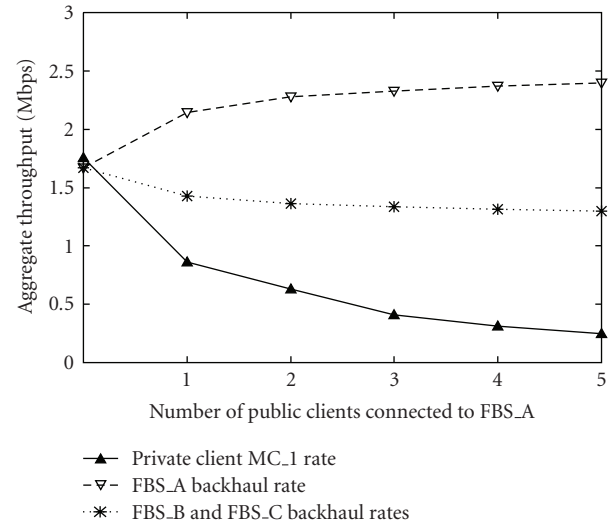

Figure 6: Private mode achievable rate versus backhaul rate. This figure shows the effects of allowing public clients to connect to an FBS. It can be seen that the achievable throughput of the private client which owns the FBS decreases as the number of public clients connecting to the FBS increases. It can also be observed that, using our compensation mechanism, the backhaul rate of the affected FBS is increased to compensate for the service to public clients.

However, at $N = 20$, there are no spectrum holes to be found and the transmission would either operate at a lower data rate (low-power) or be deferred. This results in a slow degradation of throughput performance.

In Figure 6, the effects of an open access femtocell architecture and our proposed compensation mechanism

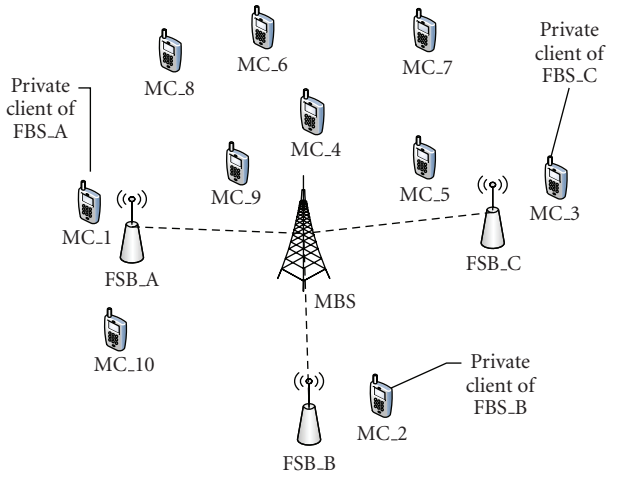

Figure 7: Simulation Scenario. In this scenario, there is 1 MBS, 3 FBSs, and 10 clients. Out of these 10 clients, 3 are private clients to an FBS. The dotted line between FBSs and MBS represents the backhaul line between them.

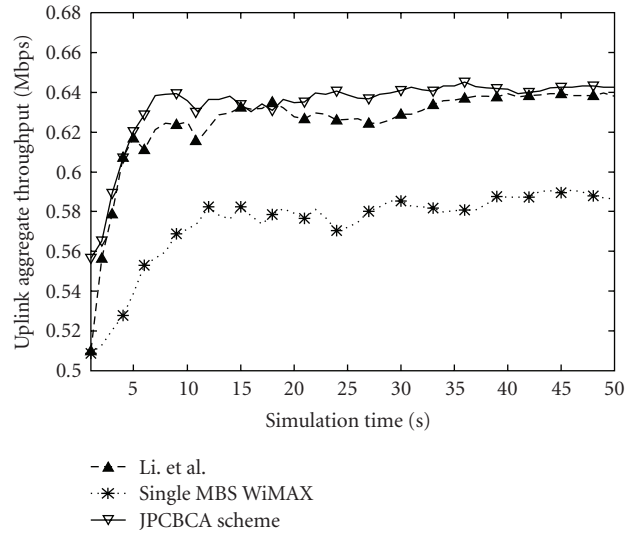

Figure 8: Uplink aggregate throughput. This figure shows that our Joint Power Control, Base Station Assignment, and Channel Assignment (JPCBCA) Scheme can achieve higher throughput as compared to the single MBS WiMAX network and the work by Li et al.

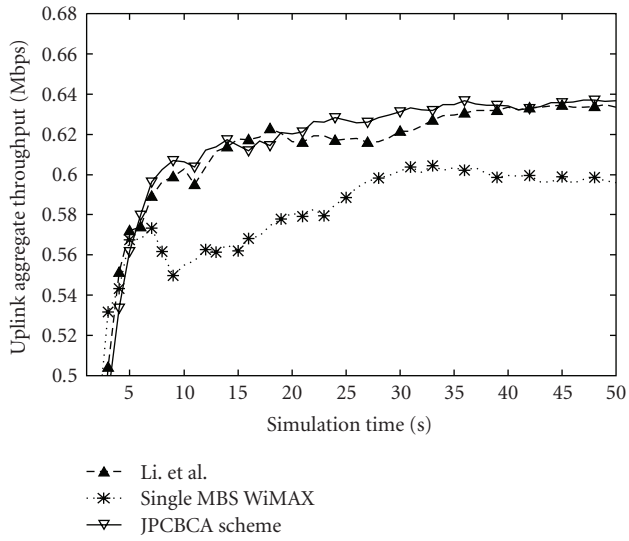

Figure 9: Downlink aggregate throughput. Similar to uplink, the throughput for the joint power control, base station assignment, and channel assignment scheme at the downlink can be seen to be better than the single MBS WiMAX network and the work by Li et al. This is due to the contention for the single MBS WiMAX network. However, for the work by Li et al., power consumption is less than that of the proposed scheme, since reduced power consumption is considered a priority in their formulation.

are investigated. We vary the public clients connected to FBS_A while FBS_B and FBS_C only service their respective private clients. As the number of public clients connecting to FBS_A is increased, the spectrum resource of FBS_A is divided between the connected public and private clients. This results in a decrease in the achievable rate for the private client MC_1, as shown in the figure. On the backhaul side, FBS_A is given additional slots for each public client that it serves, resulting in an increase in the backhaul rate. However, this also results in a decrease in the backhaul rate for the other FBSs, FBS_B and FBS_C.

The scenario for the simulation study is presented in Figure 7. There are 3 FBSs namely, FBS_A, FBS_B, and FBS_C, which are installed by private clients MC_1, MC_2, and MC_3, respectively. The public clients MC_4 to MS_10 connect to the MBS but may connect to any FBS subject to compensation. The network works under the a WiMAX environment with 2 channels available for allocation for a given time instance. The limitation of the 2 channels is necessary to assure contention for the resources for the given number of clients and base stations. Also, the MBS is capable of transmitting up to 19 Mbps while the FBSs are limited to 9 Mpbs. The joint power control, base station assignment, and channel assignment scheme is compared with the work of Li et al. [13] and a single MBS WiMAX network. The work of Li is a cognitive interference management scheme for a cognitive femtocell network architecture that chooses its transmission schedule by optimizing the channel assignment and power control.

The uplink and downlink aggregate throughput is plotted in Figures 8 and 9. It can be seen that our joint power control, base station assignment, and channel assignment scheme achieves higher throughput than the other schemes. In Li's work, the lower throughput results from connecting to the nearest BS so as to reduce power. For instance, in Figure 7, the public client MC_5 connects to FBS_C. Since FBS_C has a lower transmission rate than the MBS, the aggregate throughput decreases to a value lower than that of our scheme. The single MBS WiMAX network achieves lower throughput reading due to the contention of nodes for 2 channels.

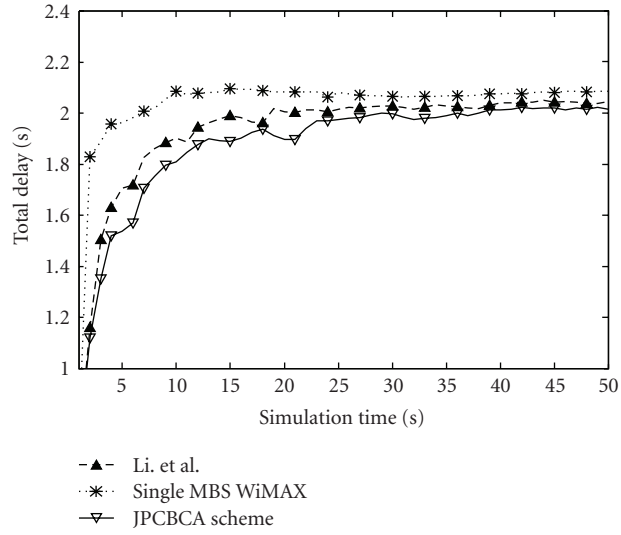

Figure 10: Delay comparison. The proposed joint power control, base station assignment, and channel assignment scheme has an average total delay of 1.8 sec. as compared to 1.9 sec. in Li et al. and 2.1 sec. in single MBS WiMAX.

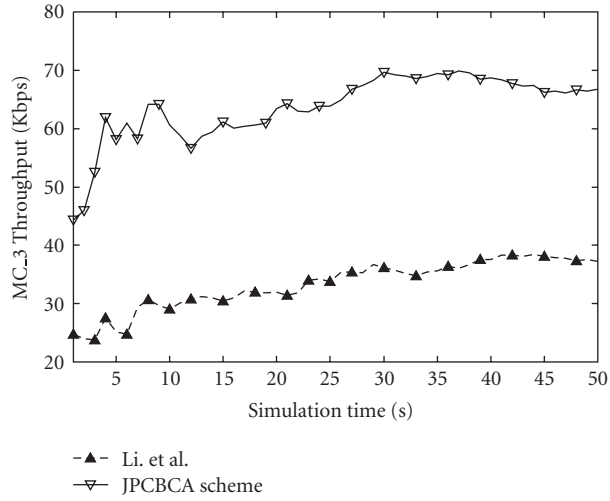

Figure 11: Private Client Throughput Comparison. This figure shows the aggregate throughput for MC_3. The throughput is higher for the joint power control, base station assignment, and channel assignment scheme since MC_5 is connected to the MBS. The client MC_5 is connected to in our scheme since the MBS is not yet in the threshold. In the event that MBS reaches its threshold, then MC_5 connects to FBS_3 in our scheme and the throughput value is the same as in Li's.

The total delay experienced by transmissions is also observed to be less for our joint power control, base station assignment, and channel assignment scheme. Figure 10 shows the improvement in the delay experienced by transmissions. The single MBS WiMAX experiences higher delay readings due to relatively more clients competing for the two channel resources as compared to Li et al. and our scheme. However, due to MC_5 connecting to FBS_C instead of the MBS, the scheme by Li results in a slightly higher delay than our Joint power control, base station assignment, and channel assignment scheme. It can also be seen in Figure 11 that the aggregate throughput of MC_3 for Li et al. is lower than that of our scheme due to the connection of MC_5 to FBS_C. This results from the difference between our scheme and Li's scheme. Since Y. Li's scheme is much more concerned with power consumption, their scheme attempts to connect to the nearest BS, either MBS or FBS. In the simulation scenario, Li's scheme would have MC_5 connected to FBS_C. This connection drastically decreases the achievable rate for MC_3. This situation is unfair to the private client MC_3, since it owns FBS_C. Although compensated through the backhaul rate, the loss of MC_3 in terms of achievable rate is higher than the gain obtained by the network as a whole.

5. Discussion of Related Works

The depletion of wireless spectrum resources is well documented in the literature. In a work by Staple and Werbach [1], the authors discussed the current status of the frequency spectrum. In addition, they also reported on current efforts to solve the problem of spectrum scarcity. One of the most recent efforts involves the use of software-defined radios with sensing capabilities, called cognitive radio. Mitola and Maguire [5] published a paper on cognitive radio in 1999, but it has only recently won attention by researchers as a viable solution to improving spectrum efficiency. A number of studies have been conducted to quantify the benefits of using cognitive radios. Srinivasa and Jafar [14] carried out a theoretical study on the throughput potential of cognitive radios using different cognitive perspectives. Several studies [15, 16] have also proposed architectures and applications for cognitive radios. The focus of these works was primarily on to how to handle base station hand-offs and decision mechanisms. In addition, research on spectrum management [6, 17, 18], power control [19], and node coordination [18] has been reported. In most of these works, the formulations are conducted for the spectrum configuration only. Fully-cognitive radios have generally not been addressed in recent works. Also, the coexistence of several cognitive radios has received little attention as compared to the minimization of interference to primary clients. Although several studies have concentrated on the interference contributions [20, 21], most either focus on cognitive radios or on primary client interference. These two concerns are addressed in our paper along with throughput improvement and coverage. Femtocell architecture [8, 22, 23] has been used to mitigate the noise in cognitive radio communications. Research on femtocells has shown that they are limited by the amount of usable bandwidth in a small area [8, 22]. However, most studies assume that adjacent FBSs would not interfere with each other. This assumption is valid for a moderately dense network. On the other hand, for a dense network, interference is unavoidable. This paper merges the cognitive capabilities with a femtocell architecture to mitigate this

drawback. The assumption of noninterfering base stations can now be validated even for the case of dense networks.

6. Conclusion

This paper focused on the congestion problem in radio frequency transmission. With continuing improvements of wireless technology, the scarcity of spectrum resources has exponentially increased. Nevertheless, most of the radio frequency spectrum bands are not efficiently utilized, especially the licensed bands.

To resolve this problem, recent studies have developed the use of cognitive radio based on Mitola's 1999 proposal. Using cognitive radio, the wasted bandwidth in licensed bands can be used by unlicensed bands as long as the primary licensed users do not utilize them. However, the benefits of using cognitive radios are dependent on the transmission behavior of the primary clients. If no spectrum holes are available, the cognitive clients cannot transmit. To overcome this problem, the use of femtocell a architecture is a good alternative. Femtocells are consumer-installed base stations that enable short-range communication indoors. The advantage of using femtocells is the capacity gain derived from minimizing the range at which they are transmitting.

In this paper, we proposed a cognitive femtocell network architecture that aims to efficiently utilize the radio frequency spectrum while meeting the service requirements of the clients. A joint power control, base station assignment, and channel assignment scheme is derived to efficiently maximize the overall throughput. Results show that significant improvements can be derived in using this architecture as the number of nodes in the network increases. This paper also demonstrated that using a compensation mechanism assures mutual benefits in sharing private clients between femtocell owners and the primary network.

Acknowledgments

This work was supported by the National Research Foundation of Korea's (NRF) grant funded by the Korean government (MEST) (no. 2009-0074938). They would also like to extend our gratitude to the anonymous reviewers and editor for their valuable comments and suggestions which improved the earlier versions of the paper.

References

[1] G. Staple and K. Werbach, "The end of spectrum scarcity," *IEEE Spectrum*, vol. 41, no. 3, pp. 48–52, 2004.

[2] D. Cabric, S. M. Mishra, and R. W. Brodersen, "Implementation issues in spectrum sensing for cognitive radios," in *Proceedings of the 38th Asilomar Conference on Signals, Systems and Computer*, vol. 1, pp. 772–776, Pacific Grove, Calif, USA, November 2004.

[3] T. A. Weiss and F. K. Jondral, "Spectrum pooling: an innovative strategy for the enhancement of spectrum efficiency," *IEEE Communications Magazine*, vol. 42, no. 3, pp. S8–S14, 2004.

[4] N. Golmie and F. Mouveaux, "Interference in the 2.4 GHz ISM band: impact on the bluetooth access control performance," in *IEEE International Conference on Communications (ICC '01)*, vol. 8, pp. 2540–2545, Helsinki, Finland, June 2001.

[5] J. Mitola III and G. Q. Maguire Jr., "Cognitive radio: making software radios more personal," *IEEE Personal Communications*, vol. 6, no. 4, pp. 13–18, 1999.

[6] I. F. Akyildiz, W.-Y. Lee, M. C. Vuran, and S. Mohanty, "A survey on spectrum management in cognitive radio networks," *IEEE Communications Magazine*, vol. 46, no. 4, pp. 40–48, 2008.

[7] I. F. Akyildiz, W.-Y. Lee, M. C. Vuran, and S. Mohanty, "NeXt generation/dynamic spectrum access/cognitive radio wireless networks: a survey," *Computer Networks*, vol. 50, no. 13, pp. 2127–2159, 2006.

[8] V. Chandrasekhar, J. G. Andrews, and A. Gatherer, "Femtocell networks: a survey," *IEEE Communications Magazine*, vol. 46, no. 9, pp. 59–67, 2008.

[9] V. Chandrasekhar and J. Andrews, "Uplink capacity and interference avoidance for two-tier femtocell networks," *IEEE Transactions on Wireless Communications*, vol. 8, no. 7, pp. 3498–3509, 2009.

[10] J. F. Kurose and K. W. Ross, *Computer Networking: A Top-Down Approach Featuring the Internet*, Pearson Education, 3rd edition, 2005.

[11] J. M. Park and S.-L. Kim, "Distributed throughput-maximization using the up- and downlink duality in wireless networks," in *Proceedings of the International Wireless Communications and Mobile Computing Conference (IWCMC '07)*, pp. 97–102, August 2007.

[12] D. P. Bertsekas, *Nonlinear Programming*, Athena Scientific, 2nd edition, 1999.

[13] Y. Li, M. Macuha, E. Sousa, T. Sato, and M. Nanri, "Cognitive interference management in 3G femtocells," in *Proceedings of the 20th Personnal, Indoor and Mobile Radio Communications Symposium (PIMRC '09)*, Tokyo, Japan, September 2009.

[14] S. Srinivasa and S. A. Jafar, "The throughput potential of cognitive radio: a theoretical perspective," in *Proceedings of the 40th Asilomar Conference on Signals, Systems and Computers*, pp. 221–225, October 2006.

[15] T. Ueda, K. Takeuchi, S. Kaneko, S. Nomura, and K. Sugiyama, "Packet switch and its impact on dynamic base station relocation in mesh networks using cognitive radio," *IEICE Transactions on Communications*, vol. E91-B, no. 1, pp. 102–109, 2008.

[16] F. Ge, Q. Chen, Y. Wang, C. W. Bostian, T. W. Rondeau, and B. Le, "Cognitive radio: from spectrum sharing to adaptive learning and reconfiguration," in *Proceedings of the IEEE Aerospace Conference*, pp. 1–10, March 2008.

[17] E. Adamopoulou, K. Demestichas, and M. Theologou, "Enhanced estimation of configuration capabilities in cognitive radio," *IEEE Communications Magazine*, vol. 46, no. 4, pp. 56–63, 2008.

[18] Z. Quan, S. Cui, and A. H. Sayed, "Optimal linear cooperation for spectrum sensing in cognitive radio networks," *IEEE Journal on Selected Topics in Signal Processing*, vol. 2, no. 1, pp. 28–40, 2008.

[19] Y. Chen, G. Yu, Z. Zhang, H.-H. Chen, and P. Qiu, "On cognitive radio networks with opportunistic power control strategies in fading channels," *IEEE Transactions on Wireless Communications*, vol. 7, no. 7, pp. 2752–2761, 2008.

[20] S. Geirhofer, L. Tong, and B. M. Sadler, "Cognitive medium access: constraining interference based on experimental models," *IEEE Journal on Selected Areas in Communications*, vol. 26, no. 1, pp. 95–105, 2008.

[21] J. O. Neel, R. Menon, A. B. MacKenzie, J. H. Reed, and R. P. Gilles, "Interference reducing networks," in *Proceedings of the 2nd International Conference on Cognitive Radio Oriented Wireless Networks and Communications (CrownCom '07)*, pp. 96–104, Orlando, Fla, USA, August 2007.

[22] H. Claussen, L. T. W. Ho, and L. G. Samuel, "Self-optimization of coverage for femtocell deployments," in *Proceedings of the 7th Annual Wireless Telecommunications Symposium (WTS '08)*, pp. 278–285, Ponoma, Calif, USA, April 2008.

[23] S. B. Kang, Y. M. Seo, Y. K. Lee, et al., "Soft QoS-based CAC scheme for WCDMA femtocell networks," in *Proceedings of the 10th International Conference on Advanced Communication Technology (ICACT '08)*, vol. 1, pp. 409–412, February 2008.